Histone deacetylase inhibitor treatment dramatically reduces cholesterol accumulation in Niemann-Pick type C1 mutant human fibroblasts

Nina H. Pipalia[a], Casey C. Cosner[b], Amy Huang[a], Anamitra Chatterjee[b], Pauline Bourbon[b], Nathan Farley[b], Paul Helquist[b,1], Olaf Wiest[b,1], and Frederick R. Maxfield[a,1,2]

[a]Department of Biochemistry, Weill Cornell Medical College, New York, NY 10065; and [b]Department of Chemistry and Biochemistry, University of Notre Dame, Notre Dame, IN 46556

Edited* by Matthew P. Scott, Stanford University/Howard Hughes Medical Institute, Stanford, CA, and approved February 24, 2011 (received for review October 4, 2010)

Niemann-Pick type C (NPC) disease is predominantly caused by mutations in the NPC1 protein that affect intracellular cholesterol trafficking and cause accumulation of unesterified cholesterol and other lipids in lysosomal storage organelles. We report the use of a series of small molecule histone deacetylase (HDAC) inhibitors in tissue culture models of NPC human fibroblasts. Some HDAC inhibitors lead to a dramatic correction in the NPC phenotype in cells with either one or two copies of the *NPC1*^{I1061T} mutation, and for several of the inhibitors, correction is associated with increased expression of NPC1 protein. Increased NPC1^{I1061T} protein levels may partially account for the correction of the phenotype, because this mutant can promote cholesterol efflux if it is delivered to late endosomes and lysosomes. The HDAC inhibitor treatment is ineffective in an NPC2 mutant human fibroblast line. Analysis of the isoform selectivity of the compounds used implicates HDAC1 and/or HDAC2 as likely targets for the observed correction, although other HDACs may also play a role. LBH589 (panobinostat) is an orally available HDAC inhibitor that crosses the blood–brain barrier and is currently in phase III clinical trials for several types of cancer. It restores cholesterol homeostasis in cultured NPC1 mutant fibroblasts to almost normal levels within 72 h when used at 40 nM. The findings that HDAC inhibitors can correct cholesterol storage defects in human NPC1 mutant cells provide the potential basis for treatment options for NPC disease.

Histone acetyl transferases (HAT) and histone deacetylases (HDAC) have gained considerable recognition because of their regulatory role in chromatin remodeling and gene transcription (1). These enzymes function in a synchronized feedback loop mechanism to mediate posttranslational acetylation and deacetylation of many types of proteins including histones, transcription factors, and chaperones, such as Hsp90 (2). The 18 HDACs that have been identified in mammals can be divided into four distinct classes based on their homology to yeast proteins (3, 4). Class I HDACs include HDAC1, -2, -3, and -8. Class II is divided in two subclasses, with IIa (containing one HDAC domain) including HDAC4, -5, -7, and -9 and class IIb (with two HDAC domains) including HDAC6 and -10. The only known representative of class IV in humans is HDAC11. Class III HDACs are structurally distinct in that they are homologous to yeast Sir2 and have NAD-dependent deacetylase activity. Although most HDACs reside in the nucleus, some are also found to shuttle between the nucleus and the cytoplasm (5).

Although the specific function of individual isoforms of HDAC or the mechanisms leading to the observed effects of inhibition are not clearly understood (6), studies have shown their diverse roles in cell proliferation, cell death (7), and tissue-specific developmental activity (8). This wide range of activities, together with the fact that HDACs have been found to be druggable targets for cancer and many other disorders (7, 9), has led to an intense research effort, including the development of inhibitors to regulate their activity. Current HDAC inhibitors (HDACi) belong to one of four structural classes: hydroxamates, cyclic peptides, aliphatic acids, or benzamides. Two HDACi [suberoylanilide hydroxamic acid (SAHA) and FK-228] have been approved for pharmaceutical use in the United States, and more than 10 are in clinical trials (10).

Niemann-Pick disease type C (NPC) is a fatal neurodegenerative lysosomal storage disorder resulting in abnormal accumulation of unesterified cholesterol, glycosphingolipids, and other lipids in late endosome/lysosomes (LE/Ly) of many cell types. The incidence is estimated between 1:120,000 and 1:50,000 live births (11). In addition to the CNS, abnormal lipid accumulation occurs in peripheral organs, leading to pathology in these tissues. Two genes, *npc1* and *npc2*, have been linked to the NPC defect, and the precise mechanisms of action of these proteins are under investigation. NPC1 is a multispanning transmembrane protein that is localized in the limiting membrane of the LE/Ly (12), and NPC2 is a soluble protein that is found in LE/Ly and is able to bind cholesterol (13). NPC2 has been shown to shuttle free cholesterol to and from membranes in vitro and to the N-terminal cholesterol-binding domain of NPC1 (14, 15).

The *NPC1*^{I1061T} mutation, which is expressed in the NPC1 mutant fibroblasts used in this study, is the most common mutation observed in NPC1 patients and represents 15–20% of all disease alleles (16, 17). NPC1 expression is subject to post-transcriptional regulation, and it was observed that NPC1^{I1061T} protein is expressed at much lower levels in NPC1 fibroblasts compared with NPC1 in WT cells (18). Studies on the processing and stability of the NPC1^{I1061T} mutant protein in human fibroblasts showed that, although the NPC1^{I1061T} protein is synthesized normally, it fails to undergo normal posttranslational glycosylation (19). Much of the NPC1^{I1061T} protein is a misfolded protein in the endoplasmic reticulum (ER), and it is subjected to proteasomal degradation. The overexpression of NPC1^{I1061T} or use of chemical chaperones rescues the NPC1 phenotype, indicating that the mutant is functional if delivered to LE/Ly (19).

Treatment options for NPC disease are limited. The only drug approved for treatment of NPC disease is Zavesca (Miglustat), which inhibits glycosphingolipid synthesis (20). This treatment slows the disease progression, but it does not reverse the damaged neurons or promote recovery of lost neurons. Therapy us-

Author contributions: N.H.P., P.H., O.W., and F.R.M. designed research; N.H.P., C.C.C., A.H., A.C., P.B., N.F., and O.W. performed research; N.H.P., C.C.C., A.C., P.B., N.F., and P.H. contributed new reagents/analytic tools; N.H.P., A.H., P.H., O.W., and F.R.M. analyzed data; and N.H.P., P.H., O.W., and F.R.M. wrote the paper.

The authors declare no conflict of interest.

*This Direct Submission article had a prearranged editor.

[1]P.H., O.W., and F.R.M. contributed equally to this work.

[2]To whom correspondence may be addressed. E-mail: frmaxfie@med.cornell.edu.

This article contains supporting information online at www.pnas.org/lookup/suppl/doi:10.1073/pnas.1014890108/-/DCSupplemental.

www.pnas.org/cgi/doi/10.1073/pnas.1014890108

ing 2-hydroxyl propyl cyclodextrin as a cholesterol transporter, which is delivered to LE/Ly and bypasses the need for NPC1 or NPC2 (21, 22), is another option that is effective in reversing the defect in cell culture and mouse and cat models (23). A limited initial human trial of cyclodextrin is currently in progress.

There has been a suggestion that there may be a connection between histone hyperacetylation and the level of NPC1 mRNA in response to cAMP (24). More recently, it was shown that cholesterol homeostasis in $NPC1^{-/-}$ mice was improved by treatment with valproic acid, a very weak HDACi (25). However, at the millimolar concentrations used, valproic acid is known to have a large number of effects and targets (26). HDACi increase the acetylation level of several nonhistone proteins, such as transcription factors, cytoskeletal proteins, and molecular chaperones (27). Therefore, the potential mechanism of HDAC inhibition on the NPC phenotype is not well-understood. Starting from our previous interest in HDACi (7, 28) and NPC disease (21, 29, 30), we investigated the effect of HDACi on cholesterol homeostasis in human NPC mutant fibroblasts.

Results

From the wide range of available HDACi, we synthesized or purchased a collection of six HDACi (Table 1 and Fig. S1) selected to provide a range of chemotypes, potencies, and selectivities: a moderately potent benzamide, CI-994; the United States Food and Drug Administration (FDA)-approved hydroxamic acid, SAHA; the potent hydroxamic acids, LBH589 and trichostatin A (TSA); and two isoform-selective HDACi, thiophene benzamide (31) and PCI-34051 (32). Human NPC1 mutant fibroblast cells GM03123 (a compound heterozygote with one allele with a *P237S* mutation and a second allele with an *I1061T* mutation) were initially treated with HDACi for 48 h at various concentrations. Free (i.e., unesterified) cholesterol levels in lysosomal storage organelles (LSOs) were determined quantitatively using an automated microscopy analysis based on the binding of the fluorescent dye, filipin, to cholesterol as described previously (30). Representative images of untreated filipin-stained WT cells (GM05659) (Fig. 1*A*) indicate no significant accumulation of free cholesterol in the LE/Ly. Filipin staining of GM03123 NPC1 mutant human fibroblast cells, treated with the vehicle control DMSO (Fig. 1*B*), shows extensive accumulation of free cholesterol in the LSOs. Most interestingly, the treatment of the GM03123 cells with either LBH589 (40 nM) (Fig. 1*C*) or TSA (120 nM) (Fig. 1*D*) resulted in dramatic correction of the NPC1 phenotype as observed by reduced filipin staining in the LSOs. The filipin labeling of unesterified cholesterol in HDACi-treated NPC1 mutant cells was comparable with filipin labeling of WT human fibroblasts.

The effect of each HDACi on GM03123 NPC1 mutant human fibroblasts was determined at varying concentrations and times. Fig. 2 shows the effects of four HDACi after 4, 24, 48, and 72 h. All data are normalized to their matched DMSO controls. None

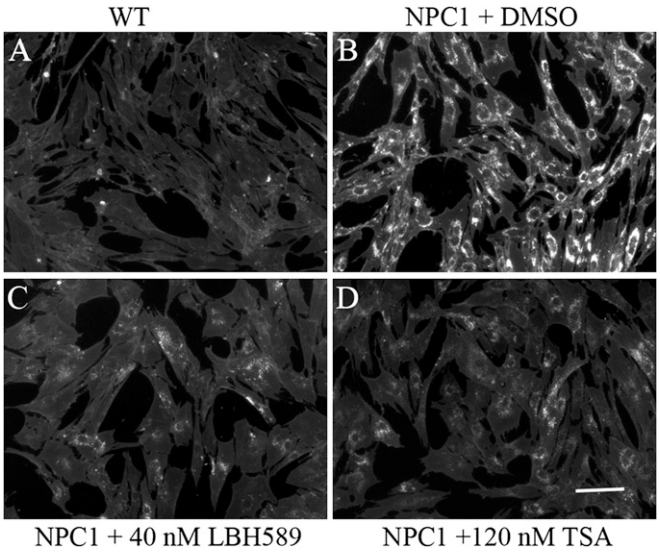

Fig. 1. Representative filipin images of HDACi-treated NPC1 mutant fibroblasts. NPC1 mutant human fibroblasts GM03123 were treated with HDACi LBH589 or 120 TSA and incubated for 48 h. Cells were subsequently fixed, stained with filipin, and imaged by epifluorescence microscopy at 10× magnification. (*A*) WT human fibroblasts GM05659. (*B*) NPC1 human fibroblasts GM03123 treated with DMSO. (*C*) GM03123 cells after 48-h treatment with 40 nM LBH589. (*D*) GM03123 cells after 48-h treatment with 120 nM TSA. (Scale bar, 25 μM.)

of the HDACi had a large effect within 4 h, but they all showed dose-dependent effects after 1 d and greater effects after 2–3 d. For CI-994 and SAHA, the EC_{50} for treatment of GM03123 cells was about 0.5 μM. For TSA, the EC_{50} was about 50 nM. LBH589 was the most potent compound, and it corrects the NPC1 phenotype with an EC_{50} below 5 nM. For both TSA and LBH589, the filipin labeling of the LSOs was indistinguishable from the WT cells at the optimal concentrations and 72 h of treatment. The effectiveness of TSA and LBH589 was reduced at higher concentrations, probably reflecting interaction with multiple targets at high doses. In summary, several HDACi are effective in correcting the NPC1 mutant phenotype, and LBH589 was the most potent inhibitor.

Encouraged by the effect of HDACi on NPC1 human fibroblasts from a donor carrying a heterozygous mutation, we investigated their efficacy on a different human NPC1 mutant fibroblast line, GM18453, in which both alleles carry the *I1061T* mutation. We also examined the HDACi effects on an NPC2 mutant human fibroblast line, GM18445, in which the donor was homozygous, with both NPC2 alleles carrying a *V39M* mutation as well as *H215R* and *I858V* homozygous polymorphisms in

Table 1. Inhibition constants K_i (μM) for the HDACi against HDAC 1–9 compared with EC_{50} (μM) in GM03123 NPC1 mutant cells

Compound\HDAC	1	2	3	4	5	6	7	8	9	EC_{50} LSO*
CI-994[†]	0.05	0.19	0.55	>20	>20	>20	>20	>20	>20	0.5
SAHA[†]	0.0013	0.0016	0.005	>20	3.6	0.0016	>20	0.48	>20	0.5
TSA[†]	0.0002	0.00065	0.005	1.4	0.26	0.001	0.195	0.045	0.8	0.05
LBH-589[‡]	0.001	0.00065	0.0011	0.55	0.08	0.0015	4.55	0.105	3.2	<0.005
Thiophene benzam[‡]	0.007	0.049	10	>10	>10	>10	>10	>10	—	0.4
PCI-34051[§]	4.0	>50	>50	—	—	2.9	—	0.01	—	>10

*Approximate concentration required for a 50% reduction in LSO filipin labeling after 48–72 h (Fig. 2 and Fig. S5).
[†]Ref. 35.
[‡]Ref. 31.
[§]Ref. 32.

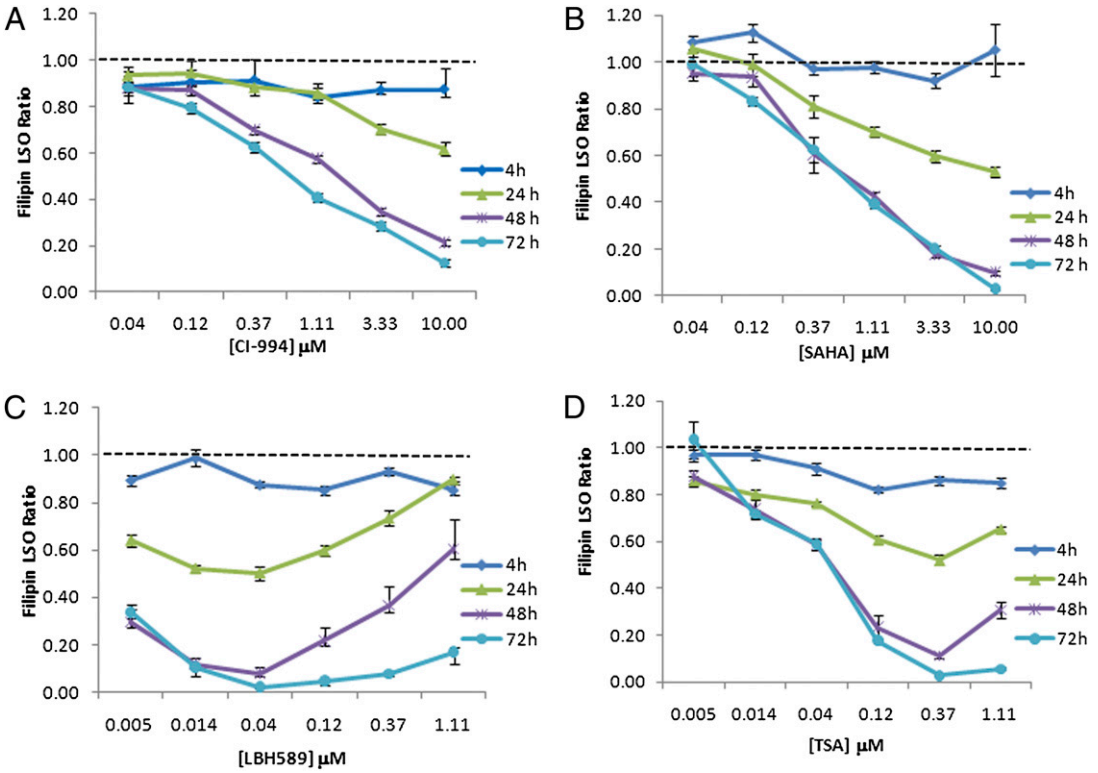

Fig. 2. Dose- and time-dependence plots for HDACi (set 1). NPC1 mutant human fibroblasts GM03123 were treated with (*A*) CI-994, (*B*) SAHA, (*C*) LBH589, or (*D*) TSA at various concentrations and for varying time followed by fixing, staining with filipin, and imaging. DMSO was used as a solvent control. Images were analyzed to obtain filipin fluorescence power in bright spots (filipin LSO ratio), and data were normalized to corresponding DMSO-treated cells. Data shown are averages of three independent experiments totaling 60 images (five wells × four sites × three experiments). The dotted horizontal lines indicate mean values for the solvent control; error bars represent SE.

NPC1. The dose dependence after 48-h treatment with four HDACi is shown in Fig. 3. Similar to the effect of HDACi on GM03123, significant correction of the NPC1 phenotype was observed on GM18453 NPC1 mutant cells. LBH589 was remarkably effective in correcting the NPC1 phenotype at 5 nM, with the highest efficacy at 40 nM (Fig. 3*A*). TSA was maximally effective at 120 nM, and both CI-994 and SAHA caused improvement in the phenotype at concentrations above 370 nM. Interestingly, none of the four HDACi tested were effective in correcting the NPC phenotype in GM18445 NPC2 mutant cells (Fig. 3*B*). Cell proliferation and cytotoxicity studies (Figs. S2 and S3) indicate that the compounds are cytostatic but not cytotoxic at the concentrations used.

We hypothesized that the mechanism of restoration of cholesterol homeostasis by HDACi might be due to the increase NPC1 expression. Protein expression levels were measured after treatment with three HDACi (SAHA, LBH589, and TSA) at their respective optimum concentrations. Fig. 4 shows analysis of NPC1 protein levels in WT cells (GM05659) and GM03123 and GM18453 NPC1 mutant cells either untreated or treated with DMSO, SAHA (10 μM), LBH589 (40 nM), or TSA (370 nM) for 48 h. NPC1 protein expression is increased after HDACi treatment in both the GM03123 and GM18453 cells. Thus, the correction of the NPC1 phenotype after HDACi treatment may be attributed, at least in part, to increased expression of NPC1 protein.

We examined the cellular mechanisms for the reduction of cholesterol in the LSOs of HDACi-treated NPC1 mutant cells. The uptake of LDL was reduced in GM03123 NPC1 mutant fibroblasts when they were treated with each of the HDACi at their optimal concentration for 48 h (Fig. 5*A* and Fig. S4). The untreated NPC1 mutant cells took up more LDL than WT GM05659 human fibroblasts, but the uptake approached the level in WT cells after treatment. Expression of the LDL receptor is regulated by sensing of cholesterol levels in the ER through the sterol-responsive element binding protein-2 (SREBP2) transcription factor, which is retained in the ER at high cholesterol levels but delivered to the Golgi and proteolyzed to release the active transcription factor at low cholesterol (33). Release of cholesterol from LSOs should restore normal delivery of cholesterol to the ER and reduce the proteolytic processing of SREBP2. As shown in Fig. 5 *B* and *C*, treatment of NPC1 mutant cells with HDACi for 18 h reduces the proteolytic processing of SREBP2, consistent with improved delivery of cholesterol to the ER.

Release of cholesterol from LE/Ly and delivery to the ER should also lead to increased cholesterol esterification by acyl Co-A:cholesterol acyl transferase (ACAT), an ER enzyme. We measured [^{14}C]-oleic acid incorporation into cholesteryl-[^{14}C]-oleate as described (34). NPC1 mutant fibroblasts GM03123 were treated with HDACi at their most effective concentration for 48 h. LBH589 treatment (40 nM) resulted in a 2.5-fold increase in ACAT-mediated esterification compared with DMSO-treated control cells (Fig. 5*D*). The induced esterification was blocked by ACAT inhibitor 58–035. SAHA, CI-994, and TSA treatment did not show a statistically significant effect. The variability in the ACAT effects may be caused by the timing of the measurement. After the HDACi treatment clears the cholesterol in the LSOs and reduces LDL uptake, it would reduce the amount of cholesterol available for esterification.

To further probe the mechanism of HDACi action, we examined which HDAC classes or isoforms might be responsible for the observed effect. Hydroxamic acids and benzamides are relatively weak inhibitors of class IIa HDACs. As shown in Table 1, LBH589,

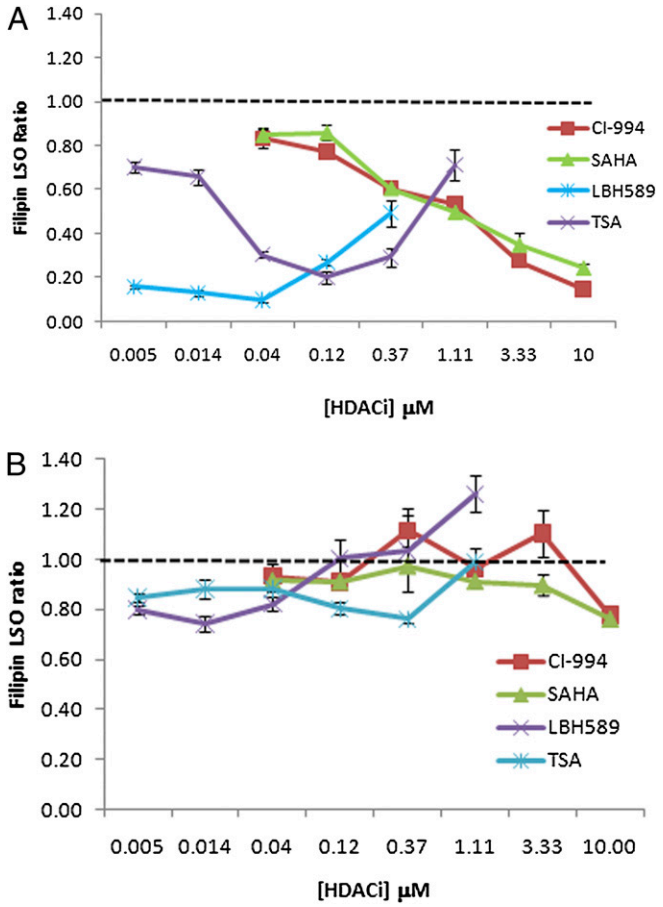

Fig. 3. Dose dependence for NPC1 mutant cells GM18453 and NPC2 mutant cells GM18445 in the presence of HDACi. NPC1 mutant human fibroblasts GM18453 (*A*) and NPC2 mutant human fibroblasts GM18445 (*B*) were treated with CI-994, SAHA, LBH589, or TSA at various concentrations for 48 h followed by fixing, staining with filipin, and imaging. DMSO was used as a solvent control. Images were analyzed to obtain filipin LSO ratio, and data were normalized to corresponding DMSO-treated cells. Data shown are averages of three independent experiments totaling 60 images (five wells × four sites × three experiments). The dotted horizontal lines indicate mean values for the solvent control; error bars represent SE.

the most potent compound in our assay, has a K_i of 1 nM to HDAC1 but 4.5 μM to HDAC7 (35). Similarly, benzamides such as CI-994 are very weak inhibitors of both class IIa and class IIb HDACs (K_i values > 20 μM). The function of class IV HDACs is presently unknown, and there are no known inhibitors available for them. Therefore, class I HDACs are left as putative targets to be studied. We tested two known isoform-selective inhibitors, PCI-34051 (an HDAC8-selective inhibitor) (32) and thiophene benzamide (an HDAC1/2-selective inhibitor) (31), on two NPC1 mutant human fibroblasts, GM03123 and GM18453. As shown in Fig. S5, there is no correction of the NPC1 phenotype by the HDAC8-selective inhibitor PCI-34051 in the 40 nM to 10 μM concentration range. In contrast, treatment with the HDAC1/2-selective inhibitor thiophene benzamide resulted in significant reduction of cholesterol accumulation in LSOs of both NPC1 mutant human fibroblast lines. These results suggest that HDAC8 is not the relevant target of less-selective HDACi, whereas HDAC1-3 inhibition may play a role in reducing the NPC phenotype.

Discussion

We report here that treatment of NPC1 mutant human fibroblasts with some HDACi at nanomolar to micromolar concentrations leads to a nearly complete clearance of the excess accumulation of cholesterol (Figs. 1–3). The lack of an effect on NPC2 mutant cells (Fig. 3*B*) indicates that the mechanism of action is not a general bypass of the NPC1- and NPC2-dependent pathways as is seen in cells treated with cholesterol-chelating cyclodextrins (21, 22). One component of the correction of the NPC phenotype is increased expression of the NPC1 protein (Fig. 4). There are several different mutations in the human NPC1 protein that are associated with NPC disease (11). The most common mutation, $NPC1^{I1061T}$, exits the ER inefficiently and is mostly degraded (19). When chaperone activity is enhanced, the $NPC1^{I1061T}$ protein can be delivered to LE/Ly, where it has sufficient activity to reverse the NPC phenotype in cultured cells (19). It is likely that several other NPC1 missense mutations would also function if sufficient amounts of the protein could pass through the ER quality control processing. We have shown that there is decreased cleavage of SREBP2 in the HDACi-treated NPC1 mutant cells. This would be expected as a consequence of release of the excess cholesterol from storage organelles as NPC1 activity is increased. The reduced SREBP2 cleavage should reduce synthesis of LDL receptors, decreasing LDL uptake (Fig. 5*A*) and thereby reducing the accumulation of LDL-derived cholesterol in LE/Ly.

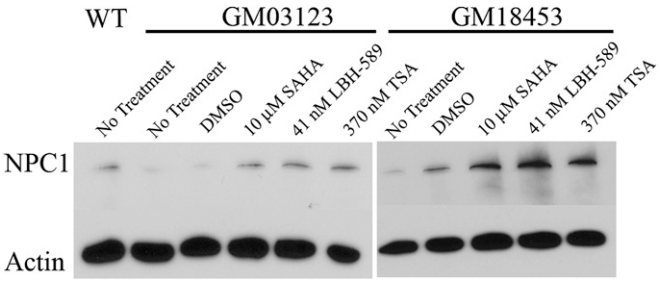

Fig. 4. Effect of HDACi on NPC1 expression. WT human fibroblast GM05659 and NPC1 mutant human fibroblasts GM03123 and GM18453 were treated with LBH589, TSA, or SAHA. As a control, cells were treated with DMSO. After 48 h, Western blot analysis was performed. The membrane was probed with mouse monoclonal anti-human NPC1 antibody, and anti–α-actin was used as a loading control.

For such mutations, a sufficient activity of the proteins in the appropriate organelles (LE/Ly) might be achieved either by making more of the protein (i.e., by increasing transcription/translation) or by increasing the efficiency of passage through the ER and Golgi apparatus. A previous report described up-regulation of the NPC1 mRNA in response to cAMP, and a mechanism involving histone acetylation was proposed (24). That study reported that treatment with TSA increased NPC1 mRNA levels in steroidogenic Y-1 cells. Recent studies have also documented induction of the 78 kDa glucose regulated protein/binding immunoglobulin protein (GRP78/BiP) and 70 kDa heat shock protein (HSP70) protein chaperones by inhibition of class I HDACs (36, 37). This suggests that HDACi could increase passage of mutant NPC1 out of the ER. Further work will be required to establish the relative contributions of these two mechanisms in increasing NPC1 expression in mutant cells.

Since the GM18453 cell line is homozygous for the $NPC1^{I1061T}$ mutation, the HDACi treatment is effective on this variant of the NPC1 protein. The GM03123 cells contain an $NPC1^{I1061T}$ allele and an $NPC1^{P237S}$ allele. It is not clear whether the expression of the P237S NPC1 protein is also increased by the HDACi treatments.

The activity of the benzamides, which are known to be inactive against class II HDACs (35), suggests that class I HDACs are responsible for the observed effects. Furthermore, the inactivity of PCI34051 excludes HDAC8 as a potential target. Although the effect of the thiophene benzamide suggests the closely related HDAC1 or HDAC2 as a target, the observed activity and selectivity of the compound is not sufficient to exclude HDAC3 as a

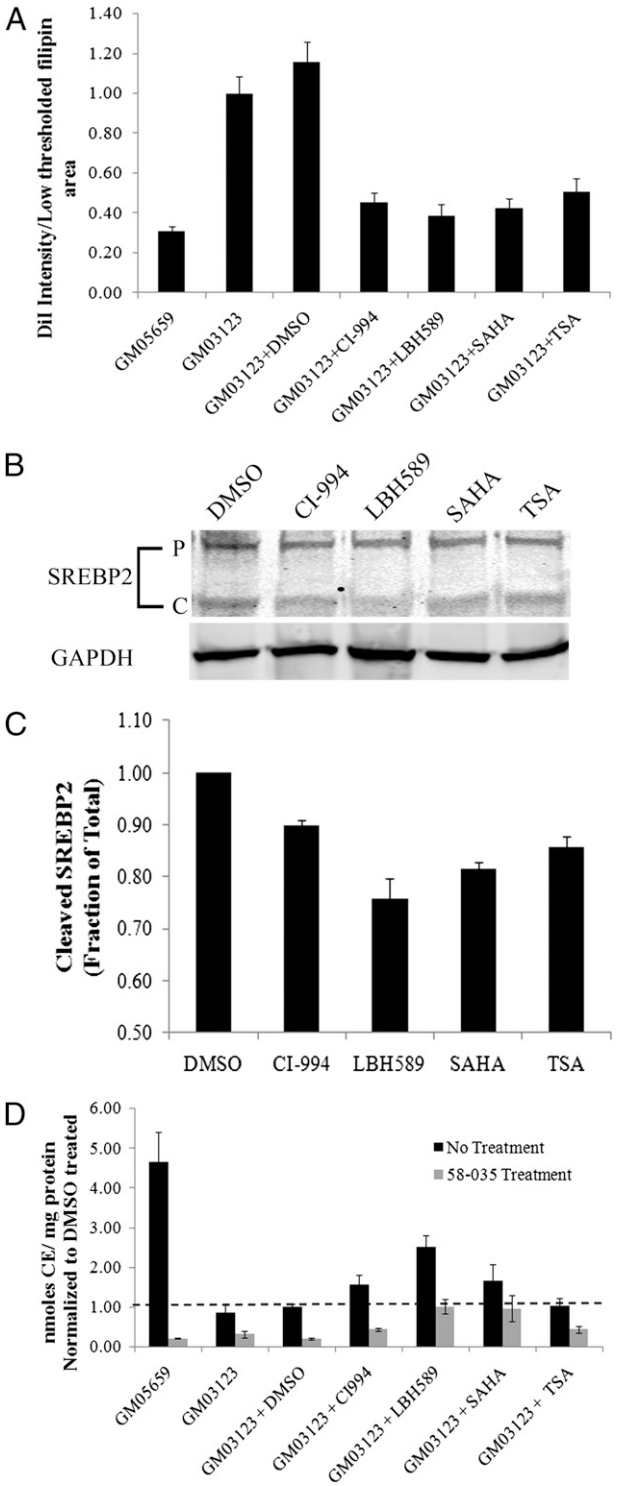

Fig. 5. Characterization of HDACi. (*A*) Dil-LDL uptake. NPC1 mutant GM03123 fibroblasts were treated with HDACi as described in *Materials and Methods*. Dil intensity per cell area was measured after treatment with 10 μM CI-994, 0.04 μM LBH589, 10 μM SAHA, or 0.37 μM TSA. DMSO treatment was used as a vehicle control, and WT GM05659 fibroblasts were used as a reference. Data shown are from three independent experiments, and 20 images were acquired per experiment. Error bar represents SE, and *P* values compared with DMSO control were <0.001 for all treatments (Student *t* test). (*B*) SREBP2 processing. GM03123 cells were treated with 10 μM CI-994, 0.04 μM LBH589, 10 μM SAHA, or 0.37 μM TSA. As a control, cells were treated with DMSO. After 18 h, Western blot analysis was performed. The membrane was probed with mouse monoclonal anti-SREBP2 antibody. (*C*) Quantification of SREBP2. The ratio of cleaved SREBP2 to total SREBP2 (precursor + cleaved form) is plotted for treatments with HDACi, using DMSO treatment as a control. Error bar represents SE, and *P* values compared with DMSO control were <0.05 for all treatments (Student *t* test). (*D*) ACAT assay. WT and NPC1 mutant GM05659 and GM03123 fibroblasts were plated in growth medium with 10% FBS at 37 °C. ACAT assay was performed as described in *Materials and Methods*. The nanomoles of cholesteryl-[^{14}C]-oleate per milligram cell protein were calculated. Data for HDACi-treated cells were normalized to DMSO-treated controls and are presented as mean ± SE. The LBH589-treated cells had a statistically significant ($P < 0.05$) increase in esterification in the absence of the ACAT inhibitor (Student Newman–Kuels multiple comparison). Two independent experiments were conducted, and each experiment had three data points.

potential target. This conclusion is analogous to the situation with the majority of the current HDACi approved or in clinical trials, which broadly inhibit HDAC1-3 (38).

The finding that treatment of NPC1 mutant fibroblasts with HDACi at submicromolar concentrations results in normalization of cholesterol homeostasis may lead to treatment options for this devastating disease, especially because many HDACi have already been studied in humans as drugs for a range of other diseases. The most potent compound found in our studies, LBH589 (panobinostat), is currently being used in several clinical trials (including phase III trials) for various forms of cancer, including glioblastomas, indicating that it can efficiently cross the blood–brain barrier (39, 40). It is orally available, has good pharmacokinetic properties, and was shown to have fewer cardiac side effects compared with many other HDACi (32, 41). Detailed pharmacokinetic data showing half-lives of up to 17 h have been published (42), and LBH589 has also been shown to be well-tolerated when administered orally (43) or i.v. (44). Investigation of this and other HDACi as therapeutics in animal models of NPC is, therefore, a promising direction to explore in further studies.

Materials and Methods

Chemical Synthesis of HDAC Inhibitors. Synthesis and characterization of all compounds are described in detail in *SI Materials and Methods*, including schemes S1–S13.

Cell Culture. Human NPC1 fibroblasts GM03123 and GM18453, as well as NPC2 fibroblasts GM 18445 (Coriell Institute), were maintained in modified Eagle medium (MEM) supplemented with 10% FBS.

Preparation of Lipoprotein-Deficient Serum and LDL. Lipoprotein-deficient serum (LPDS) was obtained from FBS adjusted to a final density of 1.2 g/mL (45). LDL was obtained from human plasma. LDL was labeled with 1,1′-dioctadecyl-3,3,3′,3′-tetramethylindocarbocyanine perchlorate (DiI; Invitrogen Corporation) as described elsewhere (46, 47).

Time- and Dose-Dependence Assay. The dose dependence of four HDACi (CI-994, SAHA, LBH589, and TSA) was determined as a function of time after 4- to 72-h treatment of NPC1 mutant fibroblasts. Measurements were made from four wells for each condition in each experiment; the experiment was repeated two times. Images were acquired at 10× magnification on an ImageXpress^{Micro} automatic fluorescence microscope at four sites per well and analyzed to obtain the LSO compartment ratio (30). Additional details are in *SI Materials and Methods*.

Fluorescence Microscopy. An ImageXpress^{Micro} imaging system from Molecular Devices equipped with a 300 W Xenon-arc lamp from Perkin-Elmer, a Nikon 10× Plan Fluor 0.3 NA objective, and a Photometrics CoolSnapHQ camera from Roper Scientific was used to acquire images. Filipin images were acquired using 377/50-nm excitation and 447/60-nm emission filters with a 415-dichroic long-pass filter. DRAQ5 images were acquired using 628/40-nm excitation and 692/40 nm-emission filters with a 669-dichroic long-pass filter.

Image Analysis. Images were analyzed to obtain the filipin LSO ratio using MetaXpress Image Analysis Software as described previously (30).

DiI-LDL Uptake. Cells were plated in growth medium supplemented with 10% FBS, and after 1 d, medium was changed to 5% LPDS. After 16–18 h, cells were treated with HDACi in medium supplemented with 5% LPDS and 20 mM Hepes. After 24 h of incubation, 5 μg/mL DiI-LDL were added to the cells and incubated for additional 24 h in the presence of the HDACi. The cell area was determined based on filipin labeling, and the average DiI intensity per cell area was measured. Additional details are in *SI Materials and Methods*.

Western Blot. Western blot analysis was performed on WT and HDACi-treated NPC1 mutant fibroblasts. Primary monoclonal anti-mouse NPC1, Actin and GAPDH antibodies were from Invitrogen. Monoclonal antiSREBP2 antibody was from Santa Cruz. Secondary antibodies were either from Pierce or Licor.

ACAT Assay. Cells were plated in Falcon 24 wells. The procedure described previously (34, 48) was followed. The number of nanomoles of cholesteryl-[^{14}C]-oleate per milligram protein was determined for each well.

ACKNOWLEDGMENTS. We thank Harold Ralph for acquiring images on an automated fluorescence microscope. We gratefully acknowledge financial support from the Ara Parseghian Medical Research Foundation (to P.H., O. W., and F.R.M.), a grant from the Charles Edison Fund (to P.H.), and Grant R37-DK27083 from the National Institutes of Health (to F.R.M.).

1. Shahbazian MD, Grunstein M (2007) Functions of site-specific histone acetylation and deacetylation. *Annu Rev Biochem* 76:75–100.
2. Budillon A, Bruzzese F, Di Gennaro E, Caraglia M (2005) Multiple-target drugs: Inhibitors of heat shock protein 90 and of histone deacetylase. *Curr Drug Targets* 6: 337–351.
3. de Ruijter AJ, van Gennip AH, Caron HN, Kemp S, van Kuilenburg AB (2003) Histone deacetylases (HDACs): Characterization of the classical HDAC family. *Biochem J* 370: 737–749.
4. Gregoretti IV, Lee YM, Goodson HV (2004) Molecular evolution of the histone deacetylase family: Functional implications of phylogenetic analysis. *J Mol Biol* 338: 17–31.
5. Dokmanovic M, Clarke C, Marks PA (2007) Histone deacetylase inhibitors: Overview and perspectives. *Mol Cancer Res* 5:981–989.
6. Witt O, Deubzer HE, Milde T, Oehme I (2009) HDAC family: What are the cancer relevant targets? *Cancer Lett* 277:8–21.
7. Wiech NL, Fisher JF, Helquist P, Wiest O (2009) Inhibition of histone deacetylases: A pharmacological approach to the treatment of non-cancer disorders. *Curr Top Med Chem* 9:257–271.
8. Xu WS, Parmigiani RB, Marks PA (2007) Histone deacetylase inhibitors: Molecular mechanisms of action. *Oncogene* 26:5541–5552.
9. Fischer A, Sananbenesi F, Wang X, Dobbin M, Tsai LH (2007) Recovery of learning and memory is associated with chromatin remodelling. *Nature* 447:178–182.
10. Tan J, Cang S, Ma Y, Petrillo RL, Liu D (2010) Novel histone deacetylase inhibitors in clinical trials as anti-cancer agents. *J Hematol Oncol* 3:5.
11. Vanier MT (2010) Niemann-Pick disease type C. *Orphanet J Rare Dis* 5:16.
12. Kwon HJ, et al. (2009) Structure of N-terminal domain of NPC1 reveals distinct subdomains for binding and transfer of cholesterol. *Cell* 137:1213–1224.
13. Friedland N, Liou HL, Lobel P, Stock AM (2003) Structure of a cholesterol-binding protein deficient in Niemann-Pick type C2 disease. *Proc Natl Acad Sci USA* 100: 2512–2517.
14. Infante RE, et al. (2008) NPC2 facilitates bidirectional transfer of cholesterol between NPC1 and lipid bilayers, a step in cholesterol egress from lysosomes. *Proc Natl Acad Sci USA* 105:15287–15292.
15. Xu Z, Farver W, Kodukula S, Storch J (2008) Regulation of sterol transport between membranes and NPC2. *Biochemistry* 47:11134–11143.
16. Davies JP, Ioannou YA (2000) Topological analysis of Niemann-Pick C1 protein reveals that the membrane orientation of the putative sterol-sensing domain is identical to those of 3-hydroxy-3-methylglutaryl-CoA reductase and sterol regulatory element binding protein cleavage-activating protein. *J Biol Chem* 275:24367–24374.
17. Millat G, et al. (1999) Niemann-Pick C1 disease: The I1061T substitution is a frequent mutant allele in patients of Western European descent and correlates with a classic juvenile phenotype. *Am J Hum Genet* 65:1321–1329.
18. Watari H, et al. (2000) Determinants of NPC1 expression and action: Key promoter regions, posttranscriptional control, and the importance of a "cysteine-rich" loop. *Exp Cell Res* 259:247–256.
19. Gelsthorpe ME, et al. (2008) Niemann-Pick type C1 I1061T mutant encodes a functional protein that is selected for endoplasmic reticulum-associated degradation due to protein misfolding. *J Biol Chem* 283:8229–8236.
20. Patterson MC, Vecchio D, Prady H, Abel L, Wraith JE (2007) Miglustat for treatment of Niemann-Pick C disease: A randomised controlled study. *Lancet Neurol* 6:765–772.
21. Rosenbaum AI, Zhang G, Warren JD, Maxfield FR (2010) Endocytosis of beta-cyclodextrins is responsible for cholesterol reduction in Niemann-Pick type C mutant cells. *Proc Natl Acad Sci USA* 107:5477–5482.
22. Abi-Mosleh L, Infante RE, Radhakrishnan A, Goldstein JL, Brown MS (2009) Cyclodextrin overcomes deficient lysosome-to-endoplasmic reticulum transport of cholesterol in Niemann-Pick type C cells. *Proc Natl Acad Sci USA* 106:19316–19321.
23. Liu B, et al. (2009) Reversal of defective lysosomal transport in NPC disease ameliorates liver dysfunction and neurodegeneration in the npc1-/- mouse. *Proc Natl Acad Sci USA* 106:2377–2382.
24. Gévry NY, Lalli E, Sassone-Corsi P, Murphy BD (2003) Regulation of niemann-pick c1 gene expression by the 3′5′-cyclic adenosine monophosphate pathway in steroidogenic cells. *Mol Endocrinol* 17:704–715.
25. Kim SJ, Lee BH, Lee YS, Kang KS (2007) Defective cholesterol traffic and neuronal differentiation in neural stem cells of Niemann-Pick type C disease improved by valproic acid, a histone deacetylase inhibitor. *Biochem Biophys Res Commun* 360: 593–599.
26. Terbach N, Williams RS (2009) Structure-function studies for the panacea, valproic acid. *Biochem Soc Trans* 37:1126–1132.
27. Konstantinopoulos PA, Karamouzis MV, Papavassiliou AG (2007) Focus on acetylation: The role of histone deacetylase inhibitors in cancer therapy and beyond. *Expert Opin Investig Drugs* 16:569–571.
28. Estiu G, et al. (2010) On the inhibition of histone deacetylase 8. *Bioorg Med Chem* 18: 4103–4110.
29. Devlin C, et al. (2010) Improvement in lipid and protein trafficking in Niemann-Pick C1 cells by correction of a secondary enzyme defect. *Traffic* 11:601–615.
30. Pipalia NH, Huang A, Ralph H, Rujoi M, Maxfield FR (2006) Automated microscopy screening for compounds that partially revert cholesterol accumulation in Niemann-Pick C cells. *J Lipid Res* 47:284–301.
31. Methot JL, et al. (2008) Exploration of the internal cavity of histone deacetylase (HDAC) with selective HDAC1/HDAC2 inhibitors (SHI-1:2). *Bioorg Med Chem Lett* 18: 973–978.
32. Balasubramanian S, et al. (2008) A novel histone deacetylase 8 (HDAC8)-specific inhibitor PCI-34051 induces apoptosis in T-cell lymphomas. *Leukemia* 22:1026–1034.
33. Horton JD, et al. (1998) Activation of cholesterol synthesis in preference to fatty acid synthesis in liver and adipose tissue of transgenic mice overproducing sterol regulatory element-binding protein-2. *J Clin Invest* 101:2331–2339.
34. Rujoi M, Pipalia NH, Maxfield FR (2010) Cholesterol pathways affected by small molecules that decrease sterol levels in Niemann-Pick type C mutant cells. *PLoS ONE* 5: e12788.
35. Bradner JE, et al. (2010) Chemical phylogenetics of histone deacetylases. *Nat Chem Biol* 6:238–243.
36. Baumeister P, Dong D, Fu Y, Lee AS (2009) Transcriptional induction of GRP78/BiP by histone deacetylase inhibitors and resistance to histone deacetylase inhibitor-induced apoptosis. *Mol Cancer Ther* 8:1086–1094.
37. Marinova Z, et al. (2009) Valproic acid induces functional heat-shock protein 70 via Class I histone deacetylase inhibition in cortical neurons: A potential role of Sp1 acetylation. *J Neurochem* 111:976–987.
38. Mack GS (2010) To selectivity and beyond. *Nat Biotechnol* 28:1259–1266.
39. Garbes L, et al. (2009) LBH589 induces up to 10-fold SMN protein levels by several independent mechanisms and is effective even in cells from SMA patients non-responsive to valproate. *Hum Mol Genet* 18:3645–3658.
40. Reardon DA (2010) Clinical trial NCT01115036, A panobinostat Presurgery (CLBH589C). Available at http://clinicaltrials.gov/ct2/show/NCT01115036.
41. Revill P, Mealy N, Seradell N, Bolos J, Rosa E (2007) Panobinostat. *Drugs Future* 32: 315–322.
42. Prince HM, Bishton MJ, Johnstone RW (2009) Panobinostat (LBH589): A potent pan-deacetylase inhibitor with promising activity against hematologic and solid tumors. *Future Oncol* 5:601–612.
43. Ellis L, et al. (2008) Histone deacetylase inhibitor panobinostat induces clinical responses with associated alterations in gene expression profiles in cutaneous T-cell lymphoma. *Clin Cancer Res* 14:4500–4510.
44. Giles F, et al. (2006) A phase I study of intravenous LBH589, a novel cinnamic hydroxamic acid analogue histone deacetylase inhibitor, in patients with refractory hematologic malignancies. *Clin Cancer Res* 12:4628–4635.
45. Goldstein JL, Basu SK, Brown MS (1983) Receptor-mediated endocytosis of low-density lipoprotein in cultured cells. *Methods Enzymol* 98:241–260.
46. Pitas RE, Innerarity TL, Weinstein JN, Mahley RW (1981) Acetoacetylated lipoproteins used to distinguish fibroblasts from macrophages in vitro by fluorescence microscopy. *Arteriosclerosis* 1:177–185.
47. Dunn KW, Maxfield FR (1992) Delivery of ligands from sorting endosomes to late endosomes occurs by maturation of sorting endosomes. *J Cell Biol* 117:301–310.
48. Rosenbaum AI, et al. (2009) Chemical screen to reduce sterol accumulation in Niemann-Pick C disease cells identifies novel lysosomal acid lipase inhibitors. *Biochim Biophys Acta* 1791:1155–1165.